ARTICLE　　　**OPEN ACCESS**

A NEURAL NETWORK CLASSIFICATION APPROACH FOR OIL SPILL DETECTION ON SAR IMAGES

Vijayakumar S[1]*, Swarnalatha P[1], and Rukmini S[2]
[1]*School of Computing Science and Engineering, VIT-University, INDIA*
[2]*Electronics and Communication Engineering (VLSI), AITS, JNTU-A, INDIA*

ABSTRACT

Synthetic Aperture Radar (SAR) is one of the coherent technique, that has been shown to have a great potential for marine surveillance applications such as oil spill and ship tracking detection. In this paper, we proposed an approach called a grey level co-occurrence matrix (GLCM) based texture feature, are applied on the SAR images to spill the oil from selected region. This uses artificial neural networks which classifies each pixel of selected region of interest (ROI) on SAR image('s). The performance development is studied by utilizing a time series of SAR images in a single ocean surface region acquired from SAR scene time series. Thereby, the remote sensing setup is trained on preliminary image of the time series and then pragmatic to consequent images from the radar satellites. After applying the classification method, the result of accuracy is at least 75% depending on the choice of our oil spill regime type. It is possible only with the radar satellite incidence projection views from the training dataset, is similar to that the classified image('s). Our proposed approach computational cost is moderately considering for classification operational procedure, near-real time service of SAR image processing.
.

*Corresponding author: Email: vkchinna5a8@gmail.com

INTRODUCTION

In generally, Synthetic Aperture Radar (SAR) imagery technique is considering for all intentions and purposes used for controlled surveillance of oil spill monitoring on coastal surface areas. The SAR imagery technique is using two types of sensors called as airborne and spaceborne sensors. However, most probably space-borne SAR surveillance is comparably independent of day-night and cloud coverage conditions. While, utilizing the SAR airborne sensors cannot be adverse under coastal weather conditions, are may simply unavailable over remote Arctic regions. But, the spaceborne SAR system can be acquire images over named regions on a regular and reliable basis. In particularly, the radar satellites are using SAR technique (such as RADARSAT, ERS, ENVISAT, etc...) have been employed to investigating and controlling for the navigational purposes. This can be monitoring for environmental conditions and environmental changes, for example, ice drift, iceberg detection, ice concentration, weather changes, oil spill detection, ship wake detection, shoreline detection, marine surrounding object identification, water quality analysis, and soon [1] – [4].

In marine environment surroundings, the oil spills spread over the sea surface regions for varying the gradation of lager oil tanker accidents, especially this type of variations are occurred the coastal beaches. As of now the oil pollution problem is a major aspect in observing the sea surface regions and marine surrounding environments. In addition, the small-scale release of oil into the sea surface regions, is recognized as a slicks and while large-scale ones are called spills [5]. However, the accurate detection of oil spill in a timely manner, would be beneficial to resource management for monitoring of oceanography. As of now, the remote sensing method is one of the most effective operation that can be performed on sea monitoring and marine environment for object identifying.

Most of the radar satellites are monitoring for coastal regions using SAR remote sensing techniques for detecting object's (i.e., oil spills). Basically, the satellite remote sensing system are two types, namely passive and active remote sensing techniques. The passive remote sensing techniques are used optical sensors, infrared/ultraviolet

COMPUTER SCIENCE

www.iioab.org

THE IIOAB JOURNAL

www.iioab.webs.com

systems, and microwave radiometer. The active remote sensing techniques are used radar satellite systems and laser fluoro-sensors [6], [7]. In the middle of these systems SAR can provide the valuable details about the region of specific location and size of the oil spill. It is due to the wide area coverage and day/night and all-weather conditional capabilities [8]. At this situation, the object identification is not accurately shown, due to the large area covering.

In generally, most of spaceborne SAR imagery systems are observing for detecting the oil spills, which is follows three steps: 1) dark spot identifying; 2) extraction of physical and geometrical features about the dark spot characteristics and properties; and 3) classify and discrimination about the dark spot as an oil spill or look-alike (i.e., internal waves, natural organics, jelly-fish areas, algae, threshold wind speed less than 3 m/s, rain cells, and kelp beds) [9], [10], [11]. Usually, these measurable features can be classifying as the performance of those operations, it can be operating based on manual or automatic methods [12] – [16]. In many existing systems are proposed the different approaches for detecting dark regions. But, most of the approaches are used manual selection method by cropping a broader area containing the dark formation [16], [17], regions such as adaptive threshold algorithms [12], [15], [18] – [20], marked point and statistical rule based thresholding methods [21], [22], wavelet based methods [23] – [25], fractal dimension estimation [26], [27], support vector machine [28], and neural networks [29] – [32].

In this paper, a fast, robust and effective automated approaches have been developed for oil spill monitoring. This approach is proposed a neural network classification algorithm that is used for achieving this goal. Before classifying the neural network segmentation capabilities have been already proofed in marine environment [33], that can be based on knowledge base system and it couldn't be tested for dark spot detection.

This paper is organized in four sections. Section II contains a description of the proposed method with their principle descriptions. In section III, a detailed description of each step in the dark-spot detection and the experimental analysis are obtained using ERS-2 SAR images. The conclusion and future scope is discussed in section IV.

METHODOLOGY

In our proposed methodology, the designing and development phase having two main difficulties, which can be occur for detection of dark spot is as: 1) the SAR imagery removes speckle noise due to its constructive and destructive inferences of reflections from sea surfaces regions of oil spill object detection and 2) the SAR image contrast between the dark region and its background can vary from specified area of image dark spot. And also, SAR image dark region vary from the local area of sea surface, and the spatial resolution of incidence angles [34], [35].

Pre-Processing

In this proposed methodology, the SAR imagery of full resolution is 1200 X 1800 pixels and each pixel is prohibitive computations of extracting feature vectors using radar technique for remote locations. And also, it has to take the textural information that is relevant feature responsible of spill type, which is contained on a wide coverage of SAR image dark region. It containing the low wind speed of radar resolution encompasses for spill type classification implementation. Designed for this analysis, we like better to choose using low resolution of the complete SAR image, that destruction subsequently applied using low-pass filtering. The consequence result of the image size in our algorithm is about 2200 X 3000 pixels [38], [44]. In some of artefacts are commonly find on SAR images, that is overlapping the regions of separate the image beams for several impedes and also any kind of texture analysis. Thus, the classification will occur on the separating of beams that encompass one full SAR image. The calibration as outlined of X-band SAR products in the manual operation accomplished to arrive at ρ_0 values according to the following formula:

$$\rho_0 = CalFactor * P^2 \sin\theta............(1)$$

Where θ is the resident frequency approach of pixel of image, P denotes the pixel arithmetical value backscatter about the intensity value, and *CalFactor* is denotes the calibration factor as per the distribution.
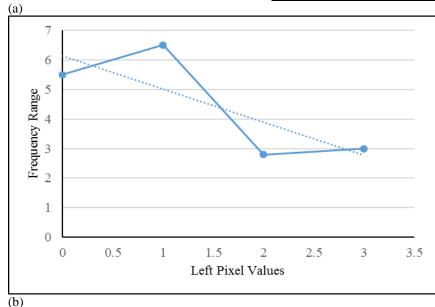
COMPUTER SCIENCE

Texture Extraction

In this analysis, the set of features are an instant feature of SAR imagery region as well as grey-level co-occurrence matrix (GLCM) features. Usually, these features are investigating for texture information and it has been explored in abundant periodicals, especially in SAR exploration [35] – [37]. Naturally, these features are containing only for first-order logic, that can be obtain the information about the image object of each grey values on each sliding window. But, the higher statistical orders can be described as usually for computing the histogram pixel values, pixel triples, etc. After this process the determination of histogram results are worked with 64 dim levels. In such a way that, we would process the enough region of interest on images for histogram results. In our numerical analysis, lower number of dark levels (e.g., 32 and 16) prompted to enhance the image that shows with less visualized pixels of interest. Such arrangements are along with these lines regarded less valuables of dark region. On account of GLCM, the first picks a parameter is based on the sliding window size.

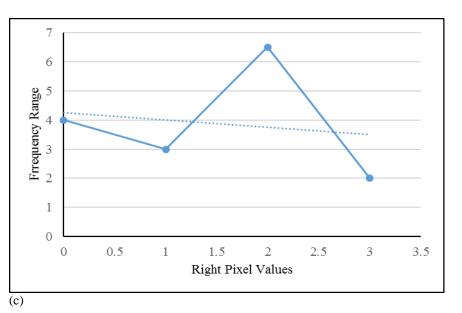| 1	2	0	0	0
1	2	0	0	0
3	1	2	0	0
3	3	1	2	1
3	1	2	1	2

(a)

(b)

(c)

Fig. 1: Grey-level co-occurrence of matrix (GLCM) illustration for 2-bit grey-level SAR image – (a) grey values in a 5X5 sliding window. (b) Resulting GLCM left pair direction, pair distance 1. (c) Resulting GLCM right pair direction, pair distance 1.

....

However, this grey-level co-occurrence matrix window (in the wake of re-binning dim qualities to, e.g., 64 dim levels) represents one of the histogram pixel set processes on SAR image region. This operation can be selected based on the image region of two neighbouring pixels, with a settled inter-pixel separation of the two pixels and altered introduction of the pair pixels [38]. The subsequent histogram operation could be done on geometric request of image pixel values, is the assumed GLCM. As half the outline for the GLCM of one 5 X 5 sliding window is shown in following **Figure- 1**.

Thus, the altered inter-pixel separation is specified image region on one of pixel, is processed from left and right pixel values. Which can be shown as the above illustration of GLCM pair axis with introduction about the image region of left and right pixel values. The other conceivable introductions for the inter-pixel separation contain no further measurable data and are subsequently not generally processed (cf., [35]). For this processing performs the operation to designing the frameworks for four bearings are then included and the subsequent grid is signified by (C (i, j)). On this joined grid (C (i, j)), we process the five normal GLCM highlights:

1) Entropy   2) dissimilarity   3) contrast   4) homogeneity   5) energy

Entropy:
$$E = -\sum_{i,j} C(i,j) \log(C(i,j)) \dots\dots\dots\dots\dots(2)$$

Contrast:
$$C = \sum_{i,j} |i-j|^2 \, C(i,j) \dots\dots\dots\dots\dots(3)$$

Dissimilarity:
$$D = \sum |i-j| \, C(i,j) \dots\dots\dots\dots\dots(4)$$

Homogeneity:
$$H = \frac{1}{1+|i-j|^2} \, C(i,j) \dots\dots\dots\dots\dots(5)$$

228

Energy: $E = \sum_{i,j} C^2(i,j)$...(6)

The texture extracting features algorithm was computed using the IDL programming language (IDL 5.0) and run on a HP Core i5 machine utilizing one CPU core. In this computation operation is performed using the ERS-2 SAR image for texture information extraction. For this analysis, each ERS-2 SAR image is computing time is up to 10 min for our texture features extraction [43]. And, its processing of all bands was near real-time results and that data processing is done through the satellite station using remote sensing techniques.

NEURAL NETWORK CLASSIFICATION

In this paper, the classification is used a neural network classifier and it has been shown without prior knowledge of data. But, the classification inconsistency is superior than the statistical methods. Especilly, it is used for dynamic neural network adoption for classification of image region. In particularly, this phenamenon is used for image region of the object detection and classification. The ocean region monitoring is a major aspect for object identifying, which is based on the part of very low gravity and gravity–capillary waves (from one centimeter to decimeteres). The locality of an oil slick on the ocean surface moistures is categories of influences in light of the echo sort conduct of the thick versatility surface movies portrayed by the Marangoni damping hypothesis [25], [29]. So, this is the vicinity of an oil slick on the ocean surface radically decreases the deliberate backscattering vitality of ocean region, bringing about darker regions in SAR symbolism. In any case, the monitoring image investigation is required in light of the fact that dim territories may likewise be created by locally low winds or by normal ocean slicks, as appeared in **Figure – 2,** where diverse concurrent occasions, which may bring about low backscattering, are noticeable.

Basically, the most of SAR image classifiers having three steps: first pre-processing the SAR image, second to extracting the features from selected SAR image region, and finally, classify the SAR image region as follows:

Step 1: In this step, we processing to remove the background of an SAR image and performs normalization opearation.

    a. Initially, it eliminates the background noise from the SAR image using region based segmentation method.
    b. And, then the SAR image size is converted for normalizing the neural network classier.

Step 2: In this step, we performing the feature extration as an oil spill or look-alike and their appropriate extraction of texture feature values.

    a. At starting of this process is proforming single-level transformation, that is narmolized image acquazation of shape and texture information from the SAR image.
    b. Then, it is based on the RGB color component model to using the image pixel intensity values.
    c. Finally, we choose the two opposite corner in SAR image region to joining, that is given for the better classification results from different texture features on image and also, this step extracting a physical feature intensity values with two appropriate points.

Step 3: finally, this step was performing the classification method based on the neural network classifier operation. For this using 12 values of physical stuctural features from the existing knowledge base system.

    a. This module performs the neural network classifier operation, that is trained from input SAR image data using the knowledge data base.

Algorithm for oil spill detection

The neural network analysis was utilized as a part of this study on looks like from the one officially depicted in [36]. A self-loader apparatus permits the extraction of some remarkable components which portray the chosen dull spot in the picture and that will be incorporated into the neural netwrok system as an information vector. These information vector elements are differenciating into three unique sorts. Some of them contains data on the backscattering force

(ascertained in dB) inclination along the outskirt of the dissected dim spot: Max Gradient (Gmax), Mean Gradient (Gme), Gradient Standard Deviation (GSD); others concentrate on the backscattering oblivious spot and/or out of sight: Object Standard Deviation (OSD), Foundation Standard Deviation (BSD), Max Contrast (ConMax), Mean Contrast (ConMe); a third classification considers the geometry and the state of the dim spot: Area (A), Perimeter (P), shape Complexity (C), Spreading (S) regarding a longitudinal hub. More exact definitions can be found in [38].
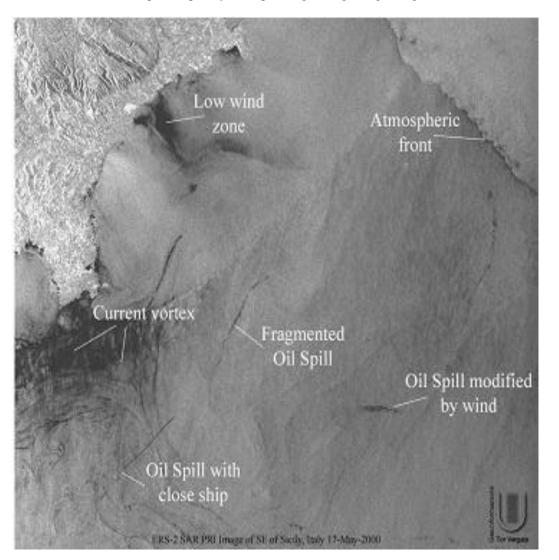

Fig: 2. Different analysis events were caused a reduction of the energy backscattering © ESA

Mainly, the ERS-2 SAR image archives over the environment of dark spot, is classified as oil spill or look-alike. For example, number of ground-truth values are available, else the discrimination was based on the independent decision making analysis of ERS-2 SAR images. The main statistical decision parameters are described from the extracted features of ERS-2 SAR image data values are show in **Table - I.**

In this proposed method, additionally considering the image object feature information is derived from the local wind speed vectors. This can be performed using backscattering gravity capillary waves and then the strong influence can appear as an oil slick on SAR image. It can be considering the wind speed conditions (i.e., less than 2-3 m/s) and it can be visualize based on the wind nature. Naturally, the wind speed is greater than 7-8 m/s and less than 15 m/s to identifying the slicks are appeared as an oil spill or look-alike. But, the wind speed computations are done by the inversion of CMOD4 model, it can be modelled by ESA to transforming the wind vectors from the ERS-2 SAR C-band measurements.

Table: I – The Main Decision Parameters in ERS-2 SAR Data about oil spill or look-alike classification

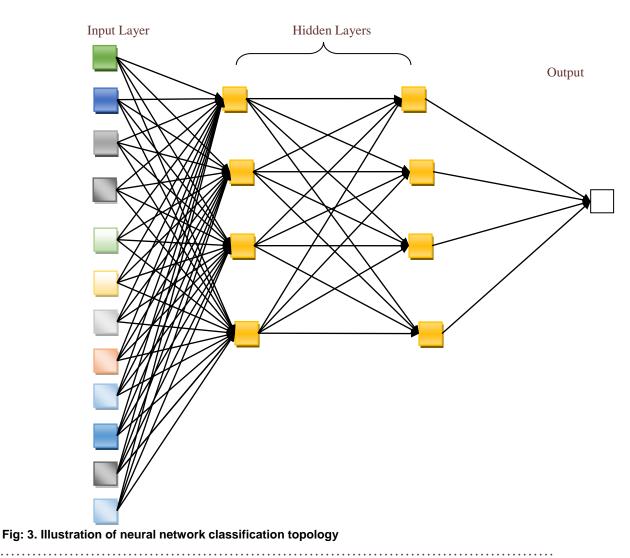| Feature	Oil Spill					Look-alike			
	Max	Min	Mean	SD		Max	Min	Mean	SD
A (Km²)	32.94	0.30	4.40	5.89		146.31	0.43	14.91	23.80
P (Km)	142.89	2.31	23.26	25.72		304.03	4.23	47.22	54.67
C	7.03	0.93	2.93	1.43		7.54	1.27	3.54	1.45
S	36.15	0.00	6.62	7.87		39.05	0.00	11.86	10.62
OSD (dB)	4.58	0.72	1.99	0.74		4.87	0.61	2.43	0.94
BSD (dB)	1.97	0.62	0.92	0.22		4.12	0.88	1.60	0.52
ConMax (dB)	17.85	4.21	9.51	3.09		18.56	4.77	12.45	2.87
ConMe (dB)	12.71	1.62	4.76	2.01		11.92	1.55	6.52	2.26
GMax (dB)	15.19	3.21	7.43	2.57		15.41	3.92	9.01	2.81
Gme (dB)	7.42	1.42	2.92	1.12		6.32	1.24	3.24	1.12
GSD (dB)	3.07	0.63	1.49	0.56		3.01	0.60	1.77	0.65
WS (m/s)	7.16	2.09	3.52	0.72		10.23	1.61	3.01	1.33

For this analysis many challenges have been initializing to accurately well excellent the number of units to be considered in the hidden layer of neural network. This topology 12-4-4-1 is shown in below **Figure - 3**. And finally this performance analysis should be in terms of both classification accuracy and training data set time.

The traditional neural network training method is as target vectors and then deciding class membership functions based on the maximum features are extracted from the selection of image region. It can be processed in the sense of the Bayesian optimal neural network classifier. Even though, the neural network assumes based on the network global weight space and its global minimum solution, that can be modelled from the specified network topology. And also, the neural network classification pattern can be considering as a non-parametric method for estimation of probabilities. This estimation process is considering the heuristic view of essential characteristics and its interpretation of level-of-confidence. From these concepts the classification confidence error estimating probability depends on the maximum occurrence of object features. These estimation processes are clearly performed on the specific network structure, hidden layer weights, as well as the dynamic learning strategies and its network topology consistency of image.

This provide a huge quantitative about the measuring directions in differentiating the input image distributions. This choice is defined as Kullback-Leibler distance strategy in [42]. And also, measuring the neural network approximation of given Bayesian classifier from specified region of image. Note, this function is differentiating the actual distance of the image region as well as image posterior knowledge base.

COMPUTER SCIENCE

Fig: 3. Illustration of neural network classification topology

However, the neural network has been trained to return 1 i.e., specifies the dark spot as an oil spill, otherwise it is a look-alike. For responsible of training dataset procedure should be stopped according to the "stopping algorithm" [38]. As indicated by this calculation, the execution of the net amid the preparation (knowledge) stage be present assessed either on the preparation set or on an alternate free approval set. In the preparation set the general error in the recovery of the right yield continues diminishing with the preparation, drawing nearer an estimation of joining. On the other hand, the error on the approval set achieves a base quality after which it will begin expanding on the off chance that we proceed with the preparation. As of now the present learning stage must be interrupted, while validation of the errors. The dependence of the error on the quantity of periods (preparing cycles) for the preparing and the approval set is appeared in **Figure- 4**.

After the preparation taking into account the learning set and applying the "early ceasing" calculation we discovered a root mean square blunder (rmse) of 0.227 on the test set (3 mis-classified samples out of 60).
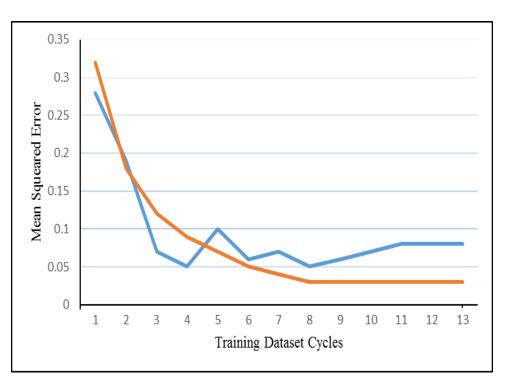
Fig: 4. The total number of training dataset cycles to be dependence of the errors for training and validation test

....

Sensitivity Analysis

As talked about in [39], the unwavering quality of the qualities for the components figured by the self-loader apparatus relies upon the capacity of the client dealing with installed edge discovery utilities. In this point of view, the sensitivity analysis completely programmed based on instruments and then the sensible analysis is assuming that the S/N proportion describing the estimations of elements might be smaller. For this situation, the determination of inputs from the neural network system, on the base of adequacy of their image data content in assessing the yield, may be prescribed to arrange of misdirecting inputs. These system operations with less inputs and has less versatile parameters to be resolved, which require a littler preparing set to be valid constraints. This system prompts are enhanced with speculation properties that giving smoother mappings. Likewise, a system with less weights may be speedier to prepare.

In the endeavour to look at which includes, in the picked setting, contain less data for the arrangement assignment we considered two routines. In a first investigation we assessed the system execution, both regarding the RMSE and the misclassification rate, for 12 distinct situations where, on turn, one of the parts of the at first considered information arrangement was absent. In a brief moment examination, we delayed the pruning system (portrayed before) to the information layer [40], [41], [42], until 11 of the 12 segments of the data vector were evaluated (we remind that an info or concealed unit is uprooted when it has lost every one of its associations).

CONCLUSION AND FUTURE WORK

This study takes after the work portrayed where the possibilities. The paper concludes with efficient results which recognises the oil spills in satellite SAR symbolism using gray level co-occurrence matrix (GLCM) based texture feature of neural networks. Thereby, the computational procedure focuses on local wind speed direction on the SAR images and provides an additional information about the ERS-2 SAR image as an input for neural networks known to evolution of the oil spills.

The future work deals with local low wind speed for knowledge based system which is significant for short gravity and the gravity-capillary waves. Finally, the low wind speed can strongly influence the appearance of the oil spill in a SAR image effectively.

REFERENCES

[1] D. Hamidi, S. Lehner, T. König, and A. Pleskachevsky, [2011] "On the sea ice motion estimation with synthetic aperture radar," in Proc. 4th TerraSAR-X Meeting, DLR, Oberpfaffenhofen, Germany, CAL0166, pp. 1–10.

[2] J. Karvonen, [2012] "Operational SAR-based sea ice drift monitoring over the Baltic Sea," Ocean Sci., vol. 8, pp. 473–483.

[3] L. Kaleschke et al., [2013] "IRO-2 Eisvorhersage und Eisrouteoptimierung," 25. Internationale Polartagung 2013-03-17. Hamburg, Germany: Deutsche Gesellschaft für Polarforschung (DGP), 22.

[4] R. Kwok, G. Spreen, and S. Pang, [2013] "Arctic sea ice circulation and drift speed: Decadal trends and ocean currents," J. Geophys. Res. Oceans, vol. 118, no. 5, pp. 2408–2425.

[5] R. H. Goodman, [1989] "Application of the Technology in the Remote Sensing of Oil Slicks", A. E. Lodge, Ed. Hoboken, NJ, USA: Wiley, 1989.

[6] M. Fingas, [2005] "The Basics of Oil Spill Cleanup. Boca Raton, FL, USA: Lewis Publ., 2001.

[7] C. Brekke and A. H. S. Solberg, "Oil spill detection by satellite remote sensing," Remote Sens. Environ., vol. 95, no. 1, pp. 1–13, Mar. 15.

[8] G. Ferraro, S. Meyer-Roux, O. Muellenhoff, M. Pavliha, J. Svetak, D. Tarchi, and K. Topouzelis, [2009] "Long term monitoring of oil spills in European seas," Int. J. Remote Sens., vol. 30, no. 3, pp. 627–645.

[9] C. Brekke and A. H. S. Solberg, [2005] "Oil spill detection by satellite remote sensing," Remote Sens. Environ., vol. 95, no. 1, pp. 1–13.

[10] A. T. Jones, M. Thankappan, G. A. Logan, J. M. Kennard, C. J. Smith, A. K. Williams, and G. M. Lawrence, [2006] "Coral spawn and bathymetric slicks in synthetic aperture radar (SAR) data from the Timor Sea, NorthWest Australia," Int. J. Remote Sens., vol. 27, no. 10, pp. 2063–2069.

[11] M. Thankappan, N. Rollet, C. J. H. Smith, A. Jones, G. Logan, and J. Kennard, [2007] "Assessment of SAR ocean features using optical and marine survey data," presented at the ENVISAT Symp., Montreux, Switzerland, Apr. 23–27.

[12] The assessment of SAR image features related Available: https://earth.esa.int/envisatsymposium/proceedings/contents.html

[13] F. Nirchio, M. Sorgente, A. Giancaspro, W. Biamino, E. Parisato, R. Ravera, and P. Trivero, [2005] "Automatic detection of oil spills from SAR images," Int. J. Remote Sens., vol. 26, no. 6, pp. 1157–1174.

[14] V. Karathanassi, K. Topouzelis, P. Pavlakis, and D. Rokos, [2006] "An objectoriented methodology to detect oil spills," Int. J. Remote Sens., vol. 27, no. 23, pp. 5235–5251.

[15] I. Keramitsoglou, C. Cartalis, and C. T. Kiranoudis, [2006] "Automatic identification of oil spills on satellite images," Environ. Modell. Softw., vol. 21, no. 5, pp. 640–652.

[16] A. H. S. Solberg, C. Brekke, and P. O. Husoy, [2007] "Oil spill detection in RADARSAT and Envisat SAR images," IEEE Trans. Geosci. Remote Sens., vol. 45, no. 3, pp. 746–755.

[17] F. Del Frate, A. Petrocchi, J. Lichtenegger, and G. Calabresi, [2000] "Neural networks for oil spill detection using ERS-SAR data," IEEE Trans. Geosci. Remote Sens., vol. 38, no. 5, pp. 2282–2287.

[18] J. Lichtenegger, G. Calabresi, and A. Petrocchi, [2000] "Detection and discrimination between oil spills and look-alike," in XIX ISPRS Congress, XXXIII, pp. 193–200.

[19] R. Solberg and N. A. Theophilopoulos, "ENVISYS—A solution for automatic oil spill detection in the Mediterranean," in Proc. 4th Int. Conf. Remote Sens. Marine Coastal Environ., 1997, pp. 3–12.

[20] A. Solberg, G. Storvik, R. Solberg, and E. Volden, [1999] "Automatic detection of oil spills in ERS SAR images," IEEE Trans. Geoci. Remote Sens., vol. 37, no. 4, pp. 1916–1924.

[21] L. Chang, Z. S. Tang, S. H. Chang, and Y. L. Chang, [2008] "A region-based GLRT detection of oil spills in SAR images," Pattern Recognit. Lett., vol. 29, no. 14, pp. 1915–1923.

[22] Y. M. Shu, J. Li, H. Yousif, and G. Gomes, [2010] "Dark-spot detection from SAR intensity imagery with spatial density thresholding for oil-spill monitoring," Remote Sens. Environ., vol. 114, no. 9, pp. 2026–2035.

[23] Y. Li and J. Li, [2010] "Oil spill detection from SAR intensity imagery using a marked point process," Remote Sens. Environ., vol. 114, no. 7, pp. 1590–1601.

[24] S. Derrode and G. Mercier, [2007] "Unsupervised multiscale oil slick segmentation from SAR images using a vector HMC model," Pattern Recognit., vol. 40, no. 3, pp. 1135–1147.

[25] S. Y. Wu and A. K. Liu, [2003] "Towards an automated ocean feature detection, extraction and classification scheme for SAR imagery," Int. J. Remote Sens., vol. 24, no. 5, pp. 935–951.

[26] A. K. Liu, C. Y. Peng, and S. Y. Chang, [1997] "Wavelet analysis of satellite images for coastal watch," IEEE J. Ocean Eng., vol. 22, no. 1, pp. 9–17.

[27] G. Benelli and A. Garzelli, [1999] "Oil-spills detection in SAR images by fractal dimension estimation," in Proc. IGARSS, Hamburg, Germany, Jun. 28–Jul. 2, pp. 218–220.

[28] M. Marghany, M. Hashim, and A. P. Cracknell, [2007] "Fractal dimension algorithm for detecting oil spills using RADARSAT-1 SAR," in Proc. LNCS, pp. 1054–1062.

[29] G Mercier and F. Girard-Ardhuin, [2006] "Partially supervised oil-slick detection by SAR imagery using kernel expansion," IEEE Trans. Geosci. Remote Sens., vol. 44, no. 10, pp. 2839–2846.

COMPUTER SCIENCE

www.iioab.org

THE IIOAB JOURNAL

www.iioab.webs.com

[30] K. Topouzelis, V. Karathanassi, P. Pavlakis, and D. Rokos, [2007] "Detection and discrimination between oil spills and look-alike phenomena through neural networks," ISPRS J. Photogramm. Remote Sens., vol. 62, no. 4, pp. 264–270.

[31] K. Topouzelis, V. Karathanassi, P. Pavlakis, and D. Rokos, [2008] "Dark formation detection using neural networks," Int. J. Remote Sens., vol. 29, no. 16, pp. 4705–4720.

[32] K. Topouzelis, D. Stathakis, and V. Karathanassi, [2009] "Investigation of genetic algorithms contribution to feature selection for oil spill detection," Int. J. Remote Sens., vol. 30, no. 3, pp. 611–625.

[33] S. Vijayakumar, V. Santhi, [2015] "Different Approaches for Oil Spill Detection in SAR Images – A Review", International Journal of Oceans and Oceanography, vol. 9, no. 2, pp. 221-228.

[34] K. N. Topouzelis, [2008] "Oil spill detection by SAR images: Dark formation detection, feature extraction and classification algorithms," Sensors, vol. 8, no. 10, pp. 6642–6659.

[35] N. Bartsch, K. Grüner, W. Keydel, and F. Witte, [1987] "Contribution to oil spill detection and analysis with radar and microwave radiometer: Results of the Archimedes II campaign," IEEE Trans. Geosci. Remote Sens., vol. GE-25, no. 6, pp. 677–690.

[36] Bogdanov, A.V.; Sandven, S.; Johannessen, O.M.; Alexandrov, V.Yu.; Bobylev, L.P., [2005] "Multisensor approach to automated classification of sea ice image data," in Geoscience and Remote Sensing, IEEE Transactions on, vol.43, no.7, pp.1648-1664.

[37] M.-A. N. Moen et al., [2013] "Comparison of automatic segmentation of full polarimetric SAR sea ice images with manually drawn ice charts," Cryosphere Discuss., vol. 7, pp. 2595–2634.

[38] C. M. Bishop, [1995] "Neural Networks for Pattern Recognition," Oxford Univ. Press.

[39] Del Frate, F.; Salvatori, L., [2004] "Oil spill detection by means of neural networks algorithms: a sensitivity analysis," in Geoscience and Remote Sensing Symposium, IGARSS '04. Proceedings. IEEE International, vol.2, no., pp.1370-1373 vol.2, pp. 20-24.

[40] Ressel, R.; Frost, A.; Lehner, S., [2015] "A Neural Network-Based Classification for Sea Ice Types on X-Band SAR Images," in Selected Topics in Applied Earth Observations and Remote Sensing, IEEE Journal of, vol.8, no.7, pp.3672-3680.

[41] Taravat, A.; Latini, D.; Del Frate, F., [2014] "Fully Automatic Dark-Spot Detection From SAR Imagery With the Combination of Nonadaptive Weibull Multiplicative Model and Pulse-Coupled Neural Networks," in Geoscience and Remote Sensing, IEEE Transactions on, vol.52, no.5, pp.2427-2435.

[42] Wan, E.A., [1990] "Neural network classification: a Bayesian interpretation," in Neural Networks, IEEE Transactions on, vol.1, no.4, pp.303-305.

[43] Prabu Sevugan, RamaKrishnan, R., Manthira Moorthi S., and Swarnalatha P., [2015] "Application of average brightness threshold algorithm for the analysis of relative radiometric correction for Ahmedabad region," International Journal of Earth Sciences and Engineering, Vol.8, Issue 1, pp.nos.341-348.

[44] Swarnalatha P, BK Tripathy,S Prabu, R Ramakrishanan and S Manthira Moorthi. [2014] "Depth Reconstruction using Geometric Correction with Anaglyph Approach for Satellite Imagery," Proceedings of International Conference on Advances in Communication, Network, and Computing, CNC, Elsevier, pp.506-515.

ABOUT AUTHORS

Singanamalla Vijayakumar received his B.Tech in Computer Science and Engineering from Vaagdevi Institute of Technology and Science ,Jawaharlal Nehru Technological University, Anantapur and M.Tech in Computer Science and Engineering from Madanapalle Institute of Technology and Science,Jawaharlal Nehru Technological University, Anantapur. Presently, he is pursuing his PhD and also working as Teaching cum Research Associate in School of Computer Science and Engineering from Vellore Institute of Technology University, Vellore, Tamil Nadu, India. He has one year teaching experience at PG level. He is doing his research work in data mining analysis and wireless network systems.

Dr. Swarnalatha P urushotham is an Associate Professor, in the School of Computer Science and Engineering, VIT University, at Vellore, India. She pursued her Ph.D degree in Image Processing and Intelligent Sstems. She has published more than 50 papers in International Journals/International Conference Proceedings/National Conferences. She is having 14+ years of teaching experiences. She is a member of IACSIT, CSI, ACM, IACSIT, IEEE (WIE), ACEEE. She is an Editorial board member/reviewer of International/ National Journals and Conferences. Her current research interest includes Image Processing, Remote Sensing, Artificial Intelligence and Software Engineering.

Rukmini Singanamalla received her B.Tech in Electronics and Communication Engineering from Vaagdevi Institute of Technology and Science, Jawaharlal Nehru Technological University, Anantapur and M.Tech in VLSI Engineering from Annamacharya Institute of Technology and Sciences, Jawaharlal Nehru Technological University, Anantapur. Presently, she is working as VLSI Design Engineer in Gray Matter Electronics Pvt. Ltd., Hyderabad, Telangana. She is doing her research work in Image Processing, Networking and VLSI system Design.

COMPUTER SCIENCE